

Journal of Materials Chemistry A

Accepted Manuscript



This is an *Accepted Manuscript*, which has been through the Royal Society of Chemistry peer review process and has been accepted for publication.

Accepted Manuscripts are published online shortly after acceptance, before technical editing, formatting and proof reading. Using this free service, authors can make their results available to the community, in citable form, before we publish the edited article. We will replace this *Accepted Manuscript* with the edited and formatted *Advance Article* as soon as it is available.

You can find more information about *Accepted Manuscripts* in the [Information for Authors](#).

Please note that technical editing may introduce minor changes to the text and/or graphics, which may alter content. The journal's standard [Terms & Conditions](#) and the [Ethical guidelines](#) still apply. In no event shall the Royal Society of Chemistry be held responsible for any errors or omissions in this *Accepted Manuscript* or any consequences arising from the use of any information it contains.



Journal Name

COMMUNICATION

A self-supported, flexible, binder-free pseudo-supercapacitor electrode material with high capacitance and cycling stability from hollow, capsular polypyrrole fibers†

Received 00th January 20xx,
Accepted 00th January 20xx

DOI: 10.1039/x0xx00000x

www.rsc.org/

Zhenyu Li,^{a,b} Jie Cai,^{a,c} Pavel Cizek,^a Haitao Niu,^a Yong Du,^a and Tong Lin^{a*}

Flexible energy devices with high performance and long-term stability are highly promising for applications in portable electronics, but remain challenging to develop. As an electrode material for pseudo supercapacitors, conducting polymers typically show higher energy storage ability over carbon materials and larger conductivity than transition-metal oxides. However conducting polymer-based supercapacitors often have poor cycling stability, attributable to the structural rupture caused by the large volume contrast between doping and de-doping states, which has been the main obstacle to their practical applications. Herein, we report a simple method to prepare flexible, binder-free, self-supported polypyrrole (PPy) supercapacitor electrode with high cycling stability through using a novel, hollow PPy nanofibers with porous capsular walls as film-forming material. The unique fiber structure and capsular walls provide the PPy film with enough free-space to adapt volume variation during doping/de-doping, leading to super-high cycling stability (capacitance retention > 90% after 11,000 charge-discharge cycles at high current density 10 A/g) and high rate capability (capacitance retention ~ 82.1 % at current density in the ranging of 0.25 A/g ~ 10 A/g).

Introduction

Enormous demand for portable personal electronics has intensified developing lightweight, high-power energy devices.¹⁻⁹ Electrochemical supercapacitors represent an advanced energy storage device with high power-density, fast charging/discharging rate, and excellent reversibility.¹⁰⁻¹⁴ In particular, flexible and wearable supercapacitors show great potential for applications in portable electronics, because of the feasibility to integrate with textile and clothing.¹⁵⁻²⁵ To this end, it is vital to develop flexible electrode materials with high capacitance performance. Free-standing electrode materials such as pure carbon films, paper-supported conducting polymers, and carbon/conducting polymer composite films have been reported.²⁶⁻³⁶

Self-standing pseudo-supercapacitor electrodes from conducting polymers have shown advantages in light-weight, flexibility and good conductivity.³⁷⁻⁴⁶ They have been reported to have higher energy storage capacity than carbon materials and larger conductivity than transition-metal oxides.⁴⁷⁻⁴⁹ Despite the wide studies, conducting polymer based electrodes often face obstacles to their practical applications. Pure conducting polymer electrodes typically suffer from poor cycling stability, attributable to the rupture originated

from large volume variation between the doped and the de-doped states which are associated with charging and discharging of the device. Consequently, pure conducting polymers based supercapacitor electrodes typically retain only up to 70% of the capacitance after 1,000 charge/discharge cycles.⁵⁸⁻⁶¹ To improve the electrode stability, conducting polymers were reinforced with a supporting material (e.g. paper,^{20,50} fabric,⁵¹ or carbon^{35,52-57}). However, the reinforcement may adversely cause issues, such as complex processing ability and reduced contact area between the supporting materials and electrolytes, though the improvement in the cycle stability.^{35, 62-65} High capacitance retention achieved by an electrode just comprising conducting polymer without external reinforcement is highly desirable but has not been reported in research literature.

In this study, we have prepared a flexible, self-standing, polypyrrole (PPy) nanofiber film that can be used directly as a supercapacitor electrode showing large specific capacitance, long cycle life and high capacitance retention. Without binder and reinforcement, the PPy film electrode has a specific capacitance of 200 F/g. Even at high current density (e.g. 10 A/g), it is still robust enough to retain at least 90% capacitance after 11,000 cycles of charge/discharge. Such unexpected stability and capacitance performance were found to stem from the unique tubular structure of PPy nanotubes which have porous capsular walls.

^aInstitute for Frontier materials, Deakin University, Geelong, Victoria 3216, Australia; Email: tong.lin@deakin.edu.au

^bAlan G. MacDiarmid Institute, Jilin University, Changchun 130012, P. R. China

^cCollege of Food Science and Technology, Huazhong Agricultural University, Wuhan 430070, China

†Electronic Supplementary Information (ESI) available: Optical images, SEM images, SEM-EDX, FTIR spectra, color change, internal resistance, and comparison of electrode cycle stability. See DOI: 10.1039/x0xx00000x

EXPERIMENTAL SECTION

Materials:

Polyvinylpyrrolidone (PVP, Mw ~1,300,000, Sigma-Aldrich), polystyrene (PS, Mw ~100,000, BDH chemical Ltd), N, N-dimethyl formamide (DMF, sigma Aldrich), vanadyl acetylacetonate (VA, 98%, Sigma-Aldrich), hydrogen chloride (37%, Sigma-Aldrich), and pyrrole (98%, Sigma Aldrich) were used as received.

Preparation of PVP/VA/PS fibers

An emulsion solution was prepared by mixing VA/PVP-DMF solution (PVP concentration 0.15 g/mL) with PS-DMF solution (PS concentration 0.2 g/mL). The volume ratio of VA/PVP-DMF to PS-DMF is 3:2 (The concentration of VA in the final mixture is 0.25 mol/L). The mixture was stirred mechanically for 12 h. Electrospinning of the emulsion solution was carried out on a needle electrospinning apparatus.⁷⁰ During electrospinning, the applied voltage, spinning distance and flow rate were controlled at 20 kV, 22 cm and 2 mL/h, respectively.

Preparation of hollow V₂O₅ fibers

The PVP/VA/PS fibers were sintered in air at 430 °C for 0.5 hour to remove any organic ingredient from the fibers and meanwhile to convert the VA to V₂O₅.

Preparation of hollow, capsular PPy fibers

Vapor-phase polymerization was conducted to generate PPy on V₂O₅ fibers. In brief, hollow V₂O₅ fiber mat was placed in a desiccator containing 2 mL of concentrated HCl in the bottom layer. The desiccator was then vacuumed for 10 min. In this way, and the V₂O₅ fibers were acidized by the HCl vapor. The acid treated V₂O₅ fibers were then placed in another desiccator filled with pyrrole (2 mL) to conduct a polymerization reaction in vacuum for 1 h. At this stage, the V₂O₅ fibers turned from yellow to dark-yellow. In the second stage, the PPy treated V₂O₅ fibers were subjected to a second acidization in HCl for 1 h and another pyrrole vapor-phase polymerization for 12 h. After the second polymerization, the final product was rinsed with HCl, deionized water and ethanol to remove the unreacted Vanadium and any side product. The film was then put into a 60 °C oven for 6 h.

Measurement of electrochemical characteristic

A two-electrode method was employed to test the electrode performance. During testing a filter paper which was soaked with 1 M aqueous H₂SO₄ solution was sandwiched with two pieces of PPy films (length 1.1 cm, width 0.8 cm, thickness 20 ± 1 μm). Two flat Pt plates were used as the current collector. The electrochemical characteristics were characterized using an electrochemistry workstation (CHI760D) at room temperature.

Characterizations

SEM and TEM images were taken on JEOL-2100 TEM with an acceleration voltage of 200 kV and Supra 55VP SEM, respectively. X-ray diffraction was measured with Scintag XDS 2000 diffractometer with Cu Kα radiation. FTIR was scanned using Bruker Vertex 70 FTIR spectrometer in ATR mode

Results and discussion

Figure 1a illustrates the procedure for preparing the hollow PPy fibers. The precursor fibers were prepared by electrospinning a dark-green emulsion solution containing PVP, VA, PS and DMF, in which PVP and VA in DMF formed the continuous phase and PS in DMF formed discontinuous phase (see ESI†). The as-spun precursor fiber mat was then subjected to a calcination treatment in air to remove polymer and organic ingredients from the fibers and meanwhile to convert the VA to V₂O₅. After calcination, yellow V₂O₅ hollow fibers with a porous wall resulted. Vapor phase polymerization was finally carried out on the hollow V₂O₅ fibers to form the PPy nanofiber film. The color change on each steps has been tracked as shown in Figure 1b.

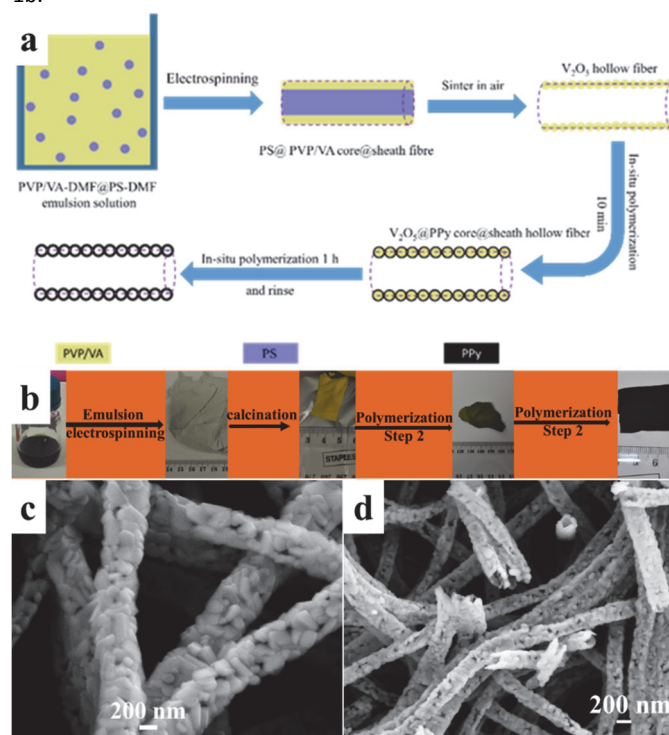


Figure 1. a) Schematic illustration of capsular nanofiber preparation, b) photos taken from each preparation steps, c) SEM top view and d) SEM cross-sectional view of porous V₂O₅ nanotubes.

Figure 1c shows the morphology of the calcined V₂O₅ nanofibers, which have a diameter of 200 ± 30 nm. The fibers had a rough surface comprising irregular nanoparticles and nano-scaled pores (see more SEM images in the ESI†). The cross-sectional image indicates that the fibers have a tubular structure with an inner diameter around 100 ± 10 nm (Figure 1d) (see more SEM images in ESI†). We also used XRD and FTIR to characterize the V₂O₅ fibers (see ESI†). The XRD diffraction peaks matched an orthorhombic phase of V₂O₅ (JCPDS No. 41-1426) with high V₂O₅ purity.

In our study, a two-step vapor-phase polymerization was employed to prepare hollow PPy nanofibers. In each step, the V₂O₅ material was treated with HCl followed by polymerization. The acid treatment in the first step was conducted in a very short period (10 min). As a result, a thin acidized layer was formed on the V₂O₅ surface. Figure 2a shows the V₂O₅ nanofibers after the first acid treatment. The acidized layer is so thin that it is almost indistinguishable. As expected, after polymerization such a thin acidized V₂O₅ layer resulted in a thin PPy layer (less than 10 nm)

between the V_2O_5 particles (see the arrowed layers in Figures 2b). The color change of V_2O_5 fibers confirmed the polymerization reaction taking place (also see more electron microscope images in ESI†).

The acid treatment and polymerization reaction in the second step were conducted in longer period (1 h and 12 h, respectively). After the second acidization and vapor-phase polymerization, the fibers almost maintained the original morphology. As shown in Figures 2c, a grain like structure is kept on the PPy fibers (Figure 2d, also see more SEM images in the ESI†). However, the TEM image indicates that the fibers have a hollow structure with lots of hollow capsules in the wall. The sheath (dark line) of the capsules was around 20 nm in thickness (see more SEM images in ESI†).

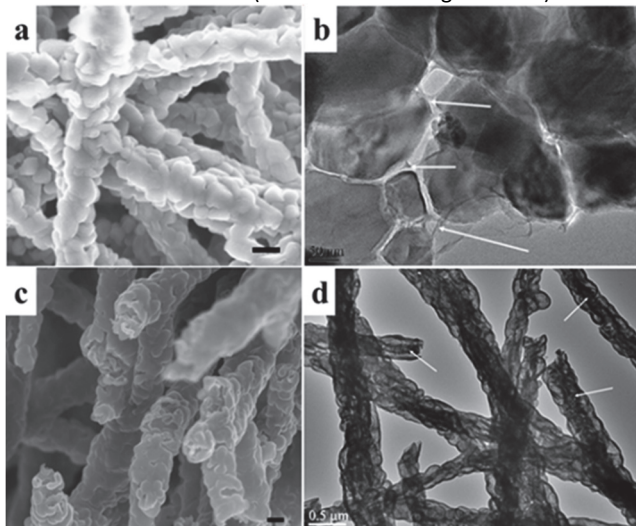


Figure 2. a) SEM image and b) TEM image of V_2O_5 fibers after the first acidization and polymerization; c) SEM image and d) TEM image of hollow, capsular PPy fibers after the second acidization and polymerization. (Scale bars in a & c: 200 nm)

It was noted that the two-step vapor-phase polymerization was essential to form the hollow capsules in the resulting PPy nanofibers. When the polymerization was conducted in one step with equivalent reaction time, hollow PPy fibers still resulted, however the wall had a dense structure without hollow capsules. Such dense wall PPy tubes were reported by the literature.⁶⁶ In our case, the thin PPy layer formed in the first polymerization step could restrict the diffusion of pyrrole vapor into the V_2O_5 phase. This leads to incomplete polymerization on the acidized V_2O_5 . When the unreacted V_2O_5 was removed by the final rinsing treatment, hollow capsules resulted. Such a capsular structure in hollow PPy is unique and has not been reported in research literature.

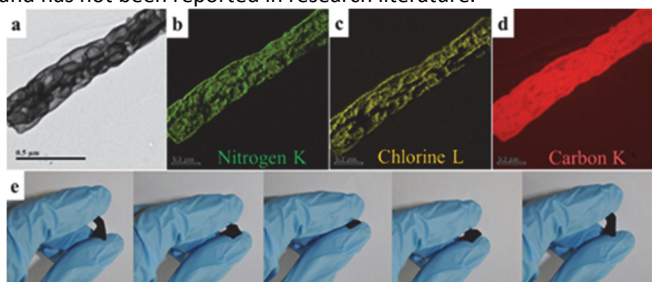


Figure 3. a) ~ d) TEM based EELS element mapping of hollow, capsular PPy fiber; e) a series of photos to illustrate the flexibility of the PPy film.

TEM based electron energy loss spectroscopy (EELS) element mapping was employed to characterize the element distribution in the PPy fibers. As shown in Figures 3a~d, elements C, N and Cl exist homogeneously in the PPy fiber sample. FTIR and SEM-EDX spectra confirmed that the fibers were PPy doped with Cl ions (see the ESI†). The PPy film obtained was flexible. It can be folded by 180° for many times without breaking, and the folded film can recover automatically (Figure 3e). Such excellent flexibility was attributed to the unique structure of the PPy film. The capsular wall with thin sheath and hollow space inside the PPy fibers provide enough free-space to endure large deformation without cracking. This remarkable structure integrity would largely facilitate the development of self-supported electrodes for supercapacitors.

To measure the electrode performance of the PPy film, we fabricated a supercapacitor device using the freestanding PPy film (without any binder) as electrode and 1 M H_2SO_4 as electrolyte. Figure 4a shows cyclic voltammetry (CV) curves in two-electrode configuration (the counter electrodes is also the reference electrode). When the device was scanned in potential window of -0.1 V to +0.7 V at a scan rate in the range of 2 mV/s ~ 200 mV/s, all the curves were approximately rectangular shapes, indicating excellent capacitive behavior and low internal resistance. Here it should be pointed out that redox peaks were not shown in the CV curves because of using two-electrode configuration for electrochemical measurement.⁶⁷⁻⁶⁹ For comparison, the CV curve in 3-electrode configuration (PPy as working electrode, a Pt wire as counter electrode and a saturated calomel electrode as reference) was also measured, which show redox peaks similar to normal PPy (see the ESI†). It was also noted that the PPy film maintained the original CV feature even if after multi-cycle of folding (see the ESI†).

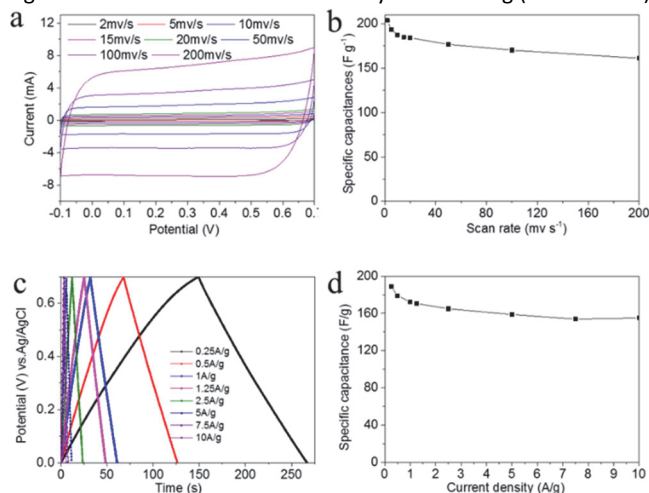


Figure 4. Capacitive performance of PPy film electrode. a) CV curves at a scan rate from 2 to 200 mV/s; b) specific capacitance change with scan rate; c) GCD curve at different current densities; d) specific capacitance change with current density.

Based on the CV curves, the specific capacitance (C_s) at different scan rates was calculated by the equation (1):

$$C_s = \frac{\int Idv}{v \times m \times \Delta V} \quad (1)$$

where I (A) is the response current, v (V/s) is the scan rate, ΔV (V) is the potential window, and m (g) is the mass of the two active

electrode material. Increasing the scan rate from 2 mV/s to 200 mV/s led to Cs change from 203 F/g to 160 F/g (Figure 4b).

Figure 4c shows the galvanostatic charge/discharge (GCD) behavior of the device, in which the charge curves are almost symmetric to their corresponding discharge counterparts in the potential window, indicating the potential of our PPy film in making supercapacitors. When the current density increased from 0.25 A/g to 10 A/g, small potential drop can be detected (see the ESI[†]), indicating the good capacitive behavior. Based on charge/discharge curves, the Cs can also be calculated by the equation (2).

$$C_s = 4 \frac{I \times \Delta t}{\Delta V \times M} \quad (2)$$

where I is the charge/discharge current, Δt is the discharge time, ΔV is potential window (V), and M is the total mass of active materials (g). Figure 4d shows the calculation result and the effect of current density on Cs.

The specific capacitance showed a slight decrease with increasing the current density from 0.25 A/g to 10 A/g. However, the capacitance value was still higher than 150 F/g when the current density was 10 A/g, proving the PPy electrode has a high rate capability (> 82%). This can be explained by the thin sheath of the capsules, which can short ion diffusion length for rapid electrochemical reaction between the electrolyte and the PPy electrode.

Figure 5a shows the electrochemical impedance spectroscopy (EIS) spectra in the frequency range of 0.01 (final) Hz to 100 KHz (initial) under 0.128 V. In the Nyquist plot, the semicircle at higher frequencies corresponds to the electron transfer limited process, whereas the linear part at lower frequencies represents the diffusion-limited electron transfer process. The linear part in the low frequency region indicated an ideal capacitive performance of the device. The solution resistance (Rs) and charge-transfer resistance (Rc) between the PPy electrode and the electrolyte were estimated, being 0.84 Ω and 36.06 Ω (inset in Figure 6a), respectively. Figure 5b shows the cycling stability result tested by GCD at a high current of 10A/g. After the first 1,000 cycles, the capacitance decreased slowly from 155 F/g to 140 F/g, and the capacitance maintained at 140 F/g in the following 10,000 cycles. Thus the capacitance retention was as high as 90.3% for the whole 11,000 cycles. After the charge/discharge cycles, the morphology of the whole PPy film did not change (see the ESI[†]). After 11,000 cycles, element sulfur was detected throughout the PPy film besides element Cl, confirming both Cl⁻ and SO₄²⁻-doping (see the ESI[†]).

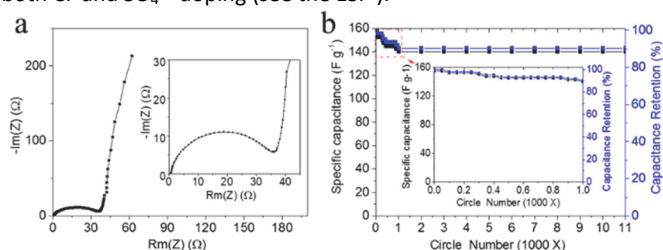


Figure 5. a) Nyquist plot of the PPy film (AC voltage of 10 mV), b) effect of charge/discharge cycles on capacitance stability and capacitance retention of PPy film electrode (current density of 10 A/g).

As reported by the previous papers,⁵⁸⁻⁶¹ structural rupture caused by the volume contrast during doping/de-doping of

conducting polymer is the main obstacle to the practical applications of conducting polymer electrode materials as supercapacitor electrode. Our PPy film offers opportunities to improve the long-term stability without using any binder and reinforcing material. Such high capacitance and excellent cycle life stem from the unique structure of PPy fiber film. Here, the capsular structures within the tubular walls of PPy fibers play two roles: (i) the large free space in the hollow fibers and within the capsules provide enough space to adapt volume variation during doping/de-doping, which significantly improves the film integrity; (ii) the thin sheath of the capsules effectively shortens ion diffusion paths, leading to fast electrochemical reaction between electrolyte and electrode. Such a unique fiber structure makes our hollow, capsular PPy fiber film surpass lots of conducting polymer-based supercapacitor electrode materials (including those with a hollow structure) in long-term cycling stability (see the data for comparison in the ESI[†]). To verify the important role of the hollow, capsular fibers in improving the cycle stability, we have also prepared normal PPy tubes without hollow capsules, and examined the film electrode performance. As expected, the device retained just 64% of the capacitance only after 1,000 cycles of charge/discharge (see detail results in the ESI[†]).

Conclusion

We have proved the excellent capacitance performance and cycling stability of a flexible, self-supported, binder-free film made of polypyrrole fibers having a novel hollow capsular structure as pseudo-supercapacitor electrode. The PPy film electrode shows high special capacitance of 203 F/g at scan rate of 2 mV/s, excellent cycling stability (capacitance retention > 90% after 11,000 charge-discharge cycles at current density of 10 A/g), and large rate capability (capacitance retention ~ 82.1 % when current density changing from 0.25 A/g to 10 A/g). Those remarkable features make our PPy film very promising for development of flexible pseudo-supercapacitor electrode. It may find applications in making flexible chemical sensors and organic solar cells.

Notes and references

- G. Gustafsson, Y. Cao, G. M. Treacy, F. Klavetter, N. Colaneri and A. J. Heeger, *Nature*, 1992, **357**, 477-479.
- K. Nomura, H. Ohta, A. Takagi, T. Kamiya, M. Hirano and H. Hosono, *Nature*, 2004, **432**, 488-492.
- Q. Cao, H. S. Kim, N. Pimparkar, J. P. Kulkarni, C. J. Wang, M. Shim, K. Roy, M. A. Alam and J. A. Rogers, *Nature*, 2008, **454**, 495-U494.
- G. Eda, G. Fanchini and M. Chhowalla, *Nat. Nanotech.*, 2008, **3**, 270-274.
- H. Nishide and K. Oyaizu, *Science*, 2008, **319**, 737-738.
- B. D. Gates, *Science*, 2009, **323**, 1566-1567.
- T. Sekitani, T. Yokota, U. Zschieschang, H. Klauk, S. Bauer, K. Takeuchi, M. Takamiya, T. Sakurai and T. Someya, *Science*, 2009, **326**, 1516-1519.
- S. Gong, W. Schwalb, Y. W. Wang, Y. Chen, Y. Tang, J. Si, B. Shirinzadeh and W. L. Cheng, *Nat. Commun.*, 2014, **5**, 3132
- M. S. Whittingham, *MRS Bull.*, 2008, **33**, 411-419.
- S. L. Rutherford and S. Lindquist, *Nature*, 1998, **396**, 336-342.
- E. Frackowiak and F. Beguin, *Carbon*, 2001, **39**, 937-950.
- A. S. Liu, R. Jones, L. Liao, D. Samara-Rubio, D. Rubin, O. Cohen, R. Nicolaescu and M. Panizza, *Nature*, 2004, **427**, 615-618.

13. J. R. Miller and P. Simon, *Science*, 2008, **321**, 651-652.
14. P. Simon and Y. Gogotsi, *Nat. Mater.*, 2008, **7**, 845-854.
15. J. Y. Ji, L. L. Zhang, H. X. Ji, Y. Li, X. Zhao, X. Bai, X. B. Fan, F. B. Zhang and R. S. Ruoff, *ACS Nano*, 2013, **7**, 6237-6243.
16. L. Q. Mai, A. Minhas-Khan, X. C. Tian, K. M. Hercule, Y. L. Zhao, X. Lin and X. Xu, *Nat. Commun.*, 2013, **4**.
17. J. Ren, W. Y. Bai, G. Z. Guan, Y. Zhang and H. S. Peng, *Adv. Mater.*, 2013, **25**, 5965-5970.
18. S. Santhanagopalan, A. Balram and D. D. Meng, *ACS Nano*, 2013, **7**, 2114-2125.
19. D. H. Seo, Z. J. Han, S. Kumar and K. Ostrikov, *Adv. Energy Mater.*, 2013, **3**, 1316-1323.
20. L. Y. Yuan, B. Yao, B. Hu, K. F. Huo, W. Chen and J. Zhou, *Energy Environ. Sci.*, 2013, **6**, 470-476.
21. F. Zhang, C. Z. Yuan, J. J. Zhu, J. Wang, X. G. Zhang and X. W. Lou, *Adv. Funct. Mater.* 2013, **23**, 3909-3915.
22. G. G. Zhang, W. F. Li, K. Y. Xie, F. Yu and H. T. Huang, *Adv. Funct. Mater.* 2013, **23**, 3675-3681.
23. J. Zhong, Z. Y. Yang, R. Mukherjee, A. V. Thomas, K. Zhu, P. Z. Sun, J. Lian, H. W. Zhu and N. Koratkar, *Nano Energy*, 2013, **2**, 1025-1030.
24. H. F. Huang, L. Q. Xu, Y. M. Tang, S. L. Tang and Y. W. Du, *Nanoscale*, 2014, **6**, 2426-2433.
25. G. Y. Zhu, Z. He, J. Chen, J. Zhao, X. M. Feng, Y. W. Ma, Q. L. Fan, L. H. Wang and W. Huang, *Nanoscale*, 2014, **6**, 1079-1085.
26. D. W. Wang, F. Li, J. P. Zhao, W. C. Ren, Z. G. Chen, J. Tan, Z. S. Wu, I. Gentle, G. Q. Lu and H. M. Cheng, *ACS Nano*, 2009, **3**, 1745-1752.
27. Q. Wu, Y. X. Xu, Z. Y. Yao, A. R. Liu and G. Q. Shi, *ACS Nano*, 2010, **4**, 1963-1970.
28. C. Z. Meng, C. H. Liu and S. S. Fan, *Electrochem. Commun.* 2009, **11**, 186-189.
29. Y. Y. Horng, Y. C. Lu, Y. K. Hsu, C. C. Chen, L. C. Chen and K. H. Chen, *J. Power Sources*, 2010, **195**, 4418-4422.
30. C. Z. Meng, C. H. Liu, L. Z. Chen, C. H. Hu and S. S. Fan, *Nano Lett.*, 2010, **10**, 4025-4031.
31. K. Jost, C. R. Perez, J. K. McDonough, V. Presser, M. Heon, G. Dion and Y. Gogotsi, *Energy Environ. Sci.*, 2011, **4**, 5060-5067.
32. L. Nyholm, G. Nystrom, A. Mihranyan and M. Stromme, *Adv. Mater.*, 2011, **23**, 3751-3769.
33. X. B. Yan, Z. X. Tai, J. T. Chen and Q. J. Xue, *Nanoscale*, 2011, **3**, 212-216.
34. F. Liu, S. Y. Song, D. F. Xue and H. J. Zhang, *Adv. Mater.*, 2012, **24**, 1089-1094.
35. H. P. Cong, X. C. Ren, P. Wang and S. H. Yu, *Energy Environ. Sci.*, 2013, **6**, 1185-1191.
36. Y. M. He, W. J. Chen, X. D. Li, Z. X. Zhang, J. C. Fu, C. H. Zhao and E. Q. Xie, *ACS Nano*, 2013, **7**, 174-182.
37. J. Jang and H. Yoon, *Chem. Commun.*, 2003, 720-721.
38. J. Jang and H. Yoon, *Langmuir*, 2005, **21**, 11484-11489.
39. X. M. Yang, Z. X. Zhu, T. Y. Dai and Y. Lu, *Macromol. Rapid Commun.* 2005, **26**, 1736-1740.
40. G. Z. Chen, M. S. P. Shaffer, D. Coleby, G. Dixon, W. Z. Zhou, D. J. Fray and A. H. Windle, *Adv. Mater.*, 2000, **12**, 522-526.
41. M. Hughes, G. Z. Chen, M. S. P. Shaffer, D. J. Fray and A. H. Windle, *Chem. Mater.*, 2002, **14**, 1610-1613.
42. M. Hughes, M. S. P. Shaffer, A. C. Renouf, C. Singh, G. Z. Chen, J. Fray and A. H. Windle, *Adv. Mater.*, 2002, **14**, 382-385.
43. H. J. Qiu, M. X. Wan, B. Matthews and L. M. Dai, *Macromolecules*, 2001, **34**, 675-677.
44. Z. X. Wei, Z. M. Zhang and M. X. Wan, *Langmuir*, 2002, **18**, 917-921.
45. L. J. Zhang and M. X. Wan, *Adv. Funct. Mater.* 2003, **13**, 815-820.
46. J. Stejskal, I. Sapurina, M. Trchova, E. N. Konyushenko and P. Holler, *Polymer*, 2006, **47**, 8253-8262.
47. G. Ciric-Marjanovic, *Synth. Met.*, 2013, **170**, 31-56.
48. H. M. Zhang and X. H. Wang, *Chin. J. Polym. Sci.*, 2013, **31**, 853-869.
49. H. X. Feng, B. Wang, L. Tan, N. L. Chen, N. X. Wang and B. Y. Chen, *J. Power Sources*, 2014, **246**, 621-628.
50. K. S. Ryu, K. M. Kim, N.-G. Park, Y. J. Park and S. H. Chang, *J. Power Sources*, 2002, **103**, 305-309.
51. H. R. Ghenaatian, M. F. Mousavi, S. H. Kazemi and M. Shamsipur, *Synth. Met.*, 2009, **159**, 1717-1722.
52. X. Du, X. Hao, Z. Wang, X. Ma, G. Guan, A. Abuliti, G. Ma and S. Liu, *Synth. Met.*, 2013, **175**, 138-145.
53. S. S. Shinde, G. S. Gund, D. P. Dubal, S. B. Jambure and C. D. Lokhande, *Electrochim. Acta*, 2014, **119**, 1-10.
54. L. Yuan, X. Xiao, T. Ding, J. Zhong, X. Zhang, Y. Shen, B. Hu, Y. Huang, J. Zhou and Z. L. Wang, *Angew. Chem. Int. Ed.*, 2012, **51**, 4934-4938.
55. K. Wang, P. Zhao, X. Zhou, H. Wu and Z. Wei, *J. Mater. Chem.*, 2011, **21**, 16373-16378.
56. A. K. Sarker and J. D. Hong, *Langmuir*, 2012, **28**, 12637-12646.
57. M. Sawangphruk, M. Suksomboon, K. Kongsupornsak, J. Khuntilo, P. Srimuk, Y. Sanguansak, P. Klunbud, P. Suktha and P. Chiochan, *J. Mater. Chem. A*, 2013, **1**, 9630-9636.
58. B. Yao, L. Y. Yuan, X. Xiao, J. Zhang, Y. Y. Qi, J. Zhou, J. Zhou, B. Hu and W. Chen, *Nano Energy*, 2013, **2**, 1071-1078.
59. J. T. Zhang, P. Chen, B. H. L. Oh and M. B. Chan-Park, *Nanoscale*, 2013, **5**, 9860-9866.
60. M. Kim, C. Lee and J. Jang, *Adv. Funct. Mater.* 2014, **24**, 2489-2499.
61. C. Y. Yang, J. L. Shen, C. Y. Wang, H. J. Fei, H. Bao and G. C. Wang, *J. Mater. Chem. A*, 2014, **2**, 1458-1464.
62. Z. Q. Niu, P. S. Luan, Q. Shao, H. B. Dong, J. Z. Li, J. Chen, D. Zhao, L. Cai, W. Y. Zhou, X. D. Chen and S. S. Xie, *Energy Environ. Sci.*, 2012, **5**, 8726-8733.
63. Y. F. Xu, M. G. Schwab, A. J. Strudwick, I. Hennig, X. L. Feng, Z. S. Wu and K. Mullen, *Adv. Energy Mater.*, 2013, **3**, 1035-1040.
64. S. Giri, D. Ghosh and C. K. Das, *Adv. Funct. Mater.* 2014, **24**, 1312-1324.
65. T. Y. Liu, L. Finn, M. H. Yu, H. Y. Wang, T. Zhai, X. H. Lu, Y. X. Tong and Y. Li, *Nano Lett.*, 2014, **14**, 2522-2527.
66. X. F. Lu, X. J. Bian, G. D. Nie, C. C. Zhang, C. Wang and Y. Wei, *J. Mater. Chem.*, 2012, **22**, 12723-12730.
67. B. Muthulakshmi, D. Kalpana, S. Pitchumani and N. G. Renganathan, *J. Power Sources*, 2006, **158**, 1533-1537.
68. R. K. Sharma, A. C. Rastogi and S. B. Desu, *Electrochem. Commun.*, 2008, **10**, 268-272.
69. W. Sun, R. Zheng and X. Chen, *J. Power Sources*, 2010, **195**, 7120-7125.
70. T. Lin, H. X. Wang, H. M. Wang and X. G. Wang, *Nanotechnology*, 2004, **15**, 1375-1381.

TOC

A hollow capsular polypyrrole nanofiber has shown great potential in preparing pseudo-supercapacitor electrode with high capacitance and excellent cycling stability.

